

# Asynchronous Distributed Variational Gaussian Processes

Hao Peng

Shandian Zhe

Yuan Qi

March 28, 2019

## Abstract

Gaussian processes (GPs) are powerful non-parametric function estimators. However, their applications are largely limited by the expensive computational cost of the inference procedures. Existing stochastic or distributed synchronous variational inferences, although have alleviated this issue by scaling up GPs to millions of samples, are still far from satisfactory for real-world large applications, where the data sizes are often orders of magnitudes larger, say, billions. To solve this problem, we propose ADVGP, the first Asynchronous Distributed Variational Gaussian Process inference implemented on the recent large-scale machine learning platform, PARAMETERSERVER. ADVGP uses a novel, general variational GP framework based on a weight space augmentation, and implements the highly efficient, asynchronous proximal gradient optimization. While maintaining comparable or better prediction performance, ADVGP greatly improves the efficiency over the existing variational inferences. With ADVGP, we effortlessly scale up GP regression to a real-world application with billions of samples and demonstrate an excellent, superior prediction performance over the popular linear models.

## 1 Introduction

Gaussian processes (GPs) (Rasmussen and Williams, 2006) are powerful non-parametric Bayesian models for function inference. Without imposing an explicit parametric form, GPs merely induce a smoothness assumption via the definition of covariance function, and hence can flexibly infer various, complicated functions from data. In addition, GPs are robust to noise, resist overfitting and produce uncertainty estimations. However, a critical bottleneck of GP models is their expensive computational cost: exact GP inference requires  $\mathcal{O}(n^3)$  time complexity and  $\mathcal{O}(n^2)$  space complexity, where  $n$  is the number of training samples; hence GPs are limited to very small applications, say, a few hundreds of samples.

To mitigate this limitation, many approximate inference algorithms have been developed (Williams and Seeger, 2001; Seeger *et al.*, 2003; Quiñero-Candela and Rasmussen, 2005; Snelson and Ghahramani, 2005; Deisenroth and Ng, 2015). Most methods use sparse approximations. That is, a small set of inducing points are introduced first; then we can develop an approximation that transfers the expensive computations of terms from the entire large training data, such as the covariance and inverse covariance matrix calculations, to the small set of the inducing points. A typical strategy is to impose some simplified modeling assumption. For example, the FITC method (Snelson and Ghahramani, 2005) assumes a fully conditionally independence. Recently, Titsias (2009) proposed a more principled, variational sparse approximation framework, where the inducing points are also treated as variational parameters. The variational framework is less prone to overfitting and often yields a better inference quality (Titsias, 2009; Bauer *et al.*, 2016). Based on the variational approximations, Hensman *et al.* (2013) developed a stochastic variational inference (SVI) algorithm, and Gal *et al.* (2014) used a tight variational lower bound to develop a distributed inference algorithm with the MAPREDUCE framework.

While SVI and distributed variational inference have successfully scaled up GP models to millions of samples ( $\mathcal{O}(10^6)$ ), they are still insufficient for real-world large-scale applications, in which the data sizes are often orders of magnitude larger, say, over billions of samples ( $\mathcal{O}(10^9)$ ). Specifically, SVI (Hensman *et al.*, 2013) sequentially processes data samples and requires too much time to complete even for one epoch of training. The distributed variational algorithm in (Gal *et al.*, 2014) uses the MAPREDUCE framework

and requires massive synchronizations during training, where a large amount of time is expended when the MAPPERS or REDUCERS are waiting for each other, or the failed nodes are restarted.

To tackle this problem, we propose Aynchronous Distributed Variational Gaussian Process inference (ADVGP), which enables GP models on applications with (at least) billions of samples. To the best of our knowledge, this is the first variational inference that scales up GPs to this level. The contributions of our work are summarized as follows: First, we derive a novel, general variational GP framework using a weight space augmentation (Section 3). The framework allows flexible choices of feature mapping functions to fulfill different variational model evidence lower bounds (ELBOs). Further, due to the simple standard normal prior of the random weights, the framework enables highly efficient, asynchronous proximal gradient-based optimization, with convergence guarantee and fast element-wise variational posterior updates. Second, based on the new framework, we develop a highly efficient, asynchronous variational inference algorithm in the recent distributed machine learning platform, PARAMETERSERVER (Li *et al.*, 2014b)(Section 4). The asynchronous algorithm eliminates an enormous amount of waiting time caused by synchronous coordination, and fully exploits computational power and network bandwidth; as a result, our new inference, ADVGP, greatly improves both the scalability and running efficiency over the existing variational inference algorithms, while still maintaining a similar or better inference quality. Finally, in a real-world application with billions of samples, we effortlessly train a GP regression model with ADVGP and demonstrate an excellent, superior predictive accuracy to the popular linear models, while existing GP models fail to handle data of such extremely large volume (Section 6).

## 2 Gaussian Processes Review

In this paper, we focus on Gaussian process (GP) regression models. Suppose we aim to infer an underlying function  $f : \mathbb{R}^d \rightarrow \mathbb{R}$  from an observed dataset  $\mathcal{D} = \{\mathbf{X}, \mathbf{y}\}$ , where  $\mathbf{X} = [\mathbf{x}_1^\top, \dots, \mathbf{x}_n^\top]^\top$  is the input matrix and  $\mathbf{y}$  is the output vector. Each row of  $\mathbf{X}$ , namely  $\mathbf{x}_i (1 \leq i \leq n)$ , is a  $d$ -dimensional input vector. Correspondingly each element of  $\mathbf{y}$ , namely  $y_i$ , is an observed function value corrupted by some random noise. Note that the function  $f$  can be highly nonlinear. To estimate  $f$  from  $\mathcal{D}$ , we place a Gaussian process prior over  $f$ . Hereafter, we treat the collection of all the function values as one realization of the GP on the function  $f$ . Therefore, the finite projection of  $f$  over the inputs  $\mathbf{X}$ , i.e.,  $\mathbf{f} = [f(\mathbf{x}_1), \dots, f(\mathbf{x}_n)]$  follows a multivariate Gaussian distribution:  $\mathbf{f} \sim \mathcal{N}(\mathbf{f}|\bar{\mathbf{f}}, \mathbf{K}_{nn})$ , where  $\bar{\mathbf{f}} = [\bar{f}(\mathbf{x}_1), \dots, \bar{f}(\mathbf{x}_n)]$  are the mean function values and  $\mathbf{K}_{nn}$  is the  $n \times n$  covariance matrix. Each element of  $\mathbf{K}_{nn}$  is a covariance function  $k(\cdot, \cdot)$  of two input vectors, i.e.,  $[\mathbf{K}_{nn}]_{i,j} = k(\mathbf{x}_i, \mathbf{x}_j)$ . We can choose any symmetric positive semidefinite kernel as the covariance function, e.g., the ARD kernel,  $k(\mathbf{x}_i, \mathbf{x}_j) = a_0^2 \exp(-\frac{1}{2}(\mathbf{x}_i - \mathbf{x}_j)^\top \text{diag}(\boldsymbol{\eta})(\mathbf{x}_i - \mathbf{x}_j))$ , where  $\boldsymbol{\eta} = [1/a_1^2, \dots, 1/a_d^2]$ . For simplicity, we usually choose the zero mean function, namely  $\bar{f}(\cdot) = 0$ .

Given  $\mathbf{f}$ , we use an isotropic Gaussian model to sample the observed noisy output  $\mathbf{y}$ :  $p(\mathbf{y}|\mathbf{f}) = \mathcal{N}(\mathbf{y}|\mathbf{f}, \beta^{-1}\mathbf{I})$ . The joint probability of the GP regression model is

$$p(\mathbf{y}, \mathbf{f}|\mathbf{X}) = \mathcal{N}(\mathbf{f}|\mathbf{0}, \mathbf{K}_{nn})\mathcal{N}(\mathbf{y}|\mathbf{f}, \beta^{-1}\mathbf{I}). \quad (1)$$

Further, we can derive the marginal distribution of  $\mathbf{y}$ , namely the model evidence, by marginalizing out  $\mathbf{f}$ :

$$p(\mathbf{y}|\mathbf{X}) = \mathcal{N}(\mathbf{y}|\mathbf{0}, \mathbf{K}_{nn} + \beta^{-1}\mathbf{I}). \quad (2)$$

The inference of the GP regression model aims to estimate the appropriate kernel parameters and noise variance from the training data  $\mathcal{D} = \{\mathbf{X}, \mathbf{y}\}$ , such as  $\{a_0, \boldsymbol{\eta}\}$  in ARD kernel and  $\beta^{-1}$ . To this end, we can maximize the model evidence in Equation (2) with respect to those parameters. However, to maximize Equation (2), we need to calculate the inverse and the determinant of the  $n \times n$  matrix  $\mathbf{K}_{nn} + \beta^{-1}\mathbf{I}$  to evaluate the multivariate Gaussian term. This will take  $\mathcal{O}(n^3)$  time complexity and  $\mathcal{O}(n^2)$  space complexity and hence is infeasible for a large number of samples,  $n$ .

For prediction, given a test input  $\mathbf{x}^*$ , since the test output  $f^*$  and training output  $\mathbf{f}$  can be treated as another GP projection on  $\mathbf{X}$  and  $\mathbf{x}^*$ , the joint distribution of  $f^*$  and  $\mathbf{f}$  is also a multivariate Gaussian distribution. Then by marginalizing out  $\mathbf{f}$ , we can obtain the posterior distribution of  $f^*$ :

$$p(f^*|\mathbf{x}^*, \mathbf{X}, \mathbf{y}) = \mathcal{N}(f^*|\alpha, v), \quad (3)$$

where

$$\alpha = \mathbf{k}_{n*}^\top (\mathbf{K}_{nn} + \beta^{-1} \mathbf{I})^{-1} \mathbf{y}, \quad (4)$$

$$v = k(x^*, x^*) - \mathbf{k}_{n*}^\top (\mathbf{K}_{nn} + \beta^{-1} \mathbf{I})^{-1} \mathbf{k}_{n*}. \quad (5)$$

and  $\mathbf{k}_{n*} = [k(\mathbf{x}^*, \mathbf{x}_1), \dots, k(\mathbf{x}^*, \mathbf{x}_n)]^\top$ . This calculation also requires the inverse of  $\mathbf{K}_{nn} + \beta^{-1} \mathbf{I}$  and hence takes  $\mathcal{O}(n^3)$  time complexity and  $\mathcal{O}(n^2)$  space complexity.

### 3 Variational Framework Using Weight Space Augmentation

Although GPs allow flexible function inference, they are severely limited by the expensive computational cost. The training and prediction both require  $\mathcal{O}(n^3)$  time complexity and  $\mathcal{O}(n^2)$  space complexity (see Equation (2), Equation (4) and Equation (5)), making GP models unrealistic for large-scale applications, where the number of samples (i.e.,  $n$ ) are often billions or even larger. To address this problem, we propose ADVGP that performs highly efficient, asynchronous distributed variational inference and enables the training of GP regression model on extremely large data. ADVGP is based on a novel variational GP framework using a weight space augmentation, which is discussed below.

We first construct an equivalent augmented model by introducing an  $m \times 1$  auxiliary random weight vector  $\mathbf{w}$  ( $m \ll n$ ). Assuming  $\mathbf{w}$  is sampled from the standard Gaussian prior distribution:  $p(\mathbf{w}) = \mathcal{N}(\mathbf{w} | \mathbf{0}, \mathbf{I})$ , with such a given  $\mathbf{w}$ , we sample an  $n \times 1$  latent function values  $\mathbf{f}$  from

$$p(\mathbf{f} | \mathbf{w}) = \mathcal{N}(\mathbf{f} | \Phi \mathbf{w}, \mathbf{K}_{nn} - \Phi \Phi^\top), \quad (6)$$

where  $\Phi$  is an  $n \times m$  matrix:  $\Phi = [\phi(\mathbf{x}_1)^\top, \dots, \phi(\mathbf{x}_n)^\top]^\top$ . Here  $\phi(\cdot)$  represents a feature mapping that maps the original  $d$ -dimensional input into an  $m$ -dimensional feature space. Note that we need to choose an appropriate  $\phi(\cdot)$  to ensure the covariance matrix in Equation (6) is symmetric positive semidefinite. Furthermore, flexible choices of  $\phi(\cdot)$  enable us to fulfill different variational model evidence lower bounds (ELBO) for large-scale inference, which we will describe in Section 5.

Given  $\mathbf{f}$ , we sample the observed output  $\mathbf{y}$  from the conditional distribution  $p(\mathbf{y} | \mathbf{f}) = \mathcal{N}(\mathbf{y} | \mathbf{f}, \beta^{-1} \mathbf{I})$ . The joint distribution of our augmented model is then given by

$$\begin{aligned} p(\mathbf{y}, \mathbf{f}, \mathbf{w} | \mathbf{X}) \\ = \mathcal{N}(\mathbf{w} | \mathbf{0}, \mathbf{I}) \mathcal{N}(\mathbf{f} | \Phi \mathbf{w}, \mathbf{K}_{nn} - \Phi \Phi^\top) \mathcal{N}(\mathbf{y} | \mathbf{f}, \beta^{-1} \mathbf{I}). \end{aligned} \quad (7)$$

This model is equivalent to the original GP regression—when we marginalize out  $\mathbf{w}$ , we recover the joint distribution in Equation (1); we can further marginalize out  $\mathbf{f}$  to recover the model evidence in Equation (2). Note that our model is different from the traditional weight space view of GP regression (Rasmussen and Williams, 2006): the feature mapping  $\phi(\cdot)$  is not equivalent to the underlying (nonlinear) feature mapping induced by the covariance function (see more discussions in Section 5). Instead,  $\phi(\cdot)$  is defined for computational purpose only, which is to construct a tractable variational evidence lower bound (ELBO), shown as follows.

Now, we derive the tractable ELBO based on the weight space augmented model in Equation (7). The derivation is similar to (Titsias, 2009; Hensman *et al.*, 2013). Specifically, we first consider the conditional distribution  $p(\mathbf{y} | \mathbf{w})$ . Because  $\log p(\mathbf{y} | \mathbf{w}) = \log \int p(\mathbf{y} | \mathbf{f}) p(\mathbf{f} | \mathbf{w}) d\mathbf{f} = \log \langle p(\mathbf{y} | \mathbf{f}) \rangle_{p(\mathbf{f} | \mathbf{w})}$ , where  $\langle \cdot \rangle_{p(\boldsymbol{\theta})}$  denotes the expectation under the distribution  $p(\boldsymbol{\theta})$ , we can use Jensen's inequality to obtain a lower bound:

$$\begin{aligned} \log p(\mathbf{y} | \mathbf{w}) &\geq \langle \log p(\mathbf{y} | \mathbf{f}) \rangle_{p(\mathbf{f} | \mathbf{w})} \\ &= \sum_{i=1}^n \log \mathcal{N}(y_i | \phi^\top(\mathbf{x}_i) \mathbf{w}, \beta^{-1}) - \frac{\beta}{2} \tilde{k}_{ii}, \end{aligned} \quad (8)$$

where  $\tilde{k}_{ii}$  is the  $i$ th diagonal element of  $\mathbf{K}_{nn} - \Phi \Phi^\top$ .

Further, we introduce a variational posterior  $q(\mathbf{w})$  to construct the variational lower bound of the log model evidence:

$$\begin{aligned}\log p(\mathbf{y}) &= \log \left\langle \frac{p(\mathbf{y}|\mathbf{w})p(\mathbf{w})}{q(\mathbf{w})} \right\rangle_{q(\mathbf{w})} \\ &\geq \langle \log p(\mathbf{y}|\mathbf{w}) \rangle_{q(\mathbf{w})} - \text{KL}(q(\mathbf{w})\|p(\mathbf{w})).\end{aligned}\quad (9)$$

where  $\text{KL}(\cdot\|\cdot)$  is the Kullback–Leibler divergence. By replacing  $\log p(\mathbf{y}|\mathbf{w})$  in Equation (9) by the right side of Equation (8), we obtain the lower bound,

$$\begin{aligned}\log p(\mathbf{y}) &\geq \mathcal{L} = -\text{KL}(q(\mathbf{w})\|p(\mathbf{w})) \\ &\quad + \sum_{i=1}^n \langle \log \mathcal{N}(y_i | \phi^\top(\mathbf{x}_i)\mathbf{w}, \beta^{-1}) \rangle_{q(\mathbf{w})} - \frac{\beta}{2} \tilde{k}_{ii}.\end{aligned}\quad (10)$$

Note that this is a variational lower bound: the equality is achieved when  $\Phi\Phi^\top = \mathbf{K}_{nn}$  and  $q(\mathbf{w}) = p(\mathbf{w}|\mathbf{y})$ . To achieve equality, we need to set  $m = n$  and the feature mapping  $\phi(\cdot)$  need to map the  $d$ -dimensional input into an  $n$ -dimensional feature space. In order to reduce the computational cost, we can restrict  $m$  to be very small and choose any family of mappings  $\phi(\cdot)$  that satisfy  $\mathbf{K}_{nn} - \Phi\Phi^\top \succeq \mathbf{0}$ . The flexible choices of  $\phi(\cdot)$  allows us to explore different approximations in a unified variational framework. For example, in our practice, we defined the feature mapping  $\phi(\cdot)$  as follows: We first introduce  $m$   $d$ -dimensional inducing points  $\{\mathbf{z}_1, \dots, \mathbf{z}_m\}$  and construct the  $m \times d$  inducing matrix  $\mathbf{Z} = [\mathbf{z}_1^\top, \dots, \mathbf{z}_m^\top]^\top$ , and then define

$$\phi(\mathbf{x}) = \mathbf{L}^\top \mathbf{k}_m(\mathbf{x}), \quad (11)$$

where  $\mathbf{k}_m(\mathbf{x}) = [k(\mathbf{x}, \mathbf{z}_1), \dots, k(\mathbf{x}, \mathbf{z}_m)]^\top$  and  $\mathbf{L}$  is the lower triangular Cholesky factorization of the inverse kernel matrix over  $\mathbf{Z}$ , i.e.,  $[\mathbf{K}_{mm}]_{i,j} = k(\mathbf{z}_i, \mathbf{z}_j)$  and  $\mathbf{K}_{mm}^{-1} = \mathbf{L}\mathbf{L}^\top$ . With some algebra, it can be verified that  $\Phi\Phi^\top = \mathbf{K}_{nm}\mathbf{K}_{mm}^{-1}\mathbf{K}_{nm}^\top$ , where  $\mathbf{K}_{nm}$  is the cross kernel matrix between  $\mathbf{X}$  and  $\mathbf{Z}$ , i.e.,  $[\mathbf{K}_{nm}]_{ij} = k(\mathbf{x}_i, \mathbf{z}_j)$ . Therefore,  $\mathbf{K}_{nn} - \Phi\Phi^\top$  is always positive semidefinite, as it can be viewed as a Schur complement of  $\mathbf{K}_{nn}$  in the matrix  $\begin{bmatrix} \mathbf{K}_{mm} & \mathbf{K}_{nm}^\top \\ \mathbf{K}_{nm} & \mathbf{K}_{nn} \end{bmatrix}$ . We discuss other choices of  $\phi(\cdot)$  in Section 5.

#### 4 Delayed Proximal Gradient Optimization for ADVGP

A particular advantage of our variational GP framework lies on its capacity to use the asynchronous, delayed proximal gradient optimization supported by PARAMETERSERVER (Li *et al.*, 2014a), with convergence guarantees and scalability to huge data. PARAMETERSERVER is a well-known, general platform for asynchronous machine learning algorithms in extremely large applications. It has a bipartite architecture where the computing nodes are partitioned into two classes: server nodes storing the model parameters and worker nodes storing the data. PARAMETERSERVER assumes the learning procedure minimizes a non-convex loss function with the following composite form:

$$L(\boldsymbol{\theta}) = \sum_{k=1}^r G_k(\boldsymbol{\theta}) + h(\boldsymbol{\theta}) \quad (12)$$

where  $\boldsymbol{\theta}$  are the model parameters. Here  $G_k(\boldsymbol{\theta})$  is a (possibly non-convex) function associated with the data in worker  $k$  and therefore can be calculated by worker  $k$  independently;  $h(\boldsymbol{\theta})$  is a convex function with respect to  $\boldsymbol{\theta}$ .

To efficiently minimize the loss function Equation (12), PARAMETERSERVER uses a delayed proximal gradient updating method to allow asynchronous optimization. To illustrate it, we first review the standard proximal gradient descent method. Specifically, for every iteration  $t$ , we first take a gradient descent step according to  $\sum_k G_k(\boldsymbol{\theta})$  and then perform a proximal operation to project  $\boldsymbol{\theta}$  toward the minimum of  $h(\cdot)$ ,

i.e.,  $\boldsymbol{\theta}^{(t+1)} = \text{Prox}_{\gamma_t}[\boldsymbol{\theta}^{(t)} - \gamma_t \sum_k \nabla G_k(\boldsymbol{\theta}^{(t)})]$ , where  $\gamma_t$  is the step size and  $\nabla G_k(\boldsymbol{\theta}^{(t)})$  is the gradient of  $G_k(\boldsymbol{\theta}^{(t)})$ . The proximal operation with respect to  $h$  is defined by

$$\text{Prox}_{\gamma_t}[\boldsymbol{\theta}] = \underset{\boldsymbol{\theta}^*}{\text{argmin}} \quad h(\boldsymbol{\theta}^*) + \frac{1}{2\gamma_t} \|\boldsymbol{\theta}^* - \boldsymbol{\theta}\|_2^2. \quad (13)$$

Although the standard proximal gradient descent guarantees to find a local minimum solution, the computation is inefficient, even in parallel: in each iteration, the server nodes wait until the worker nodes finish calculating every  $\nabla G_k(\boldsymbol{\theta}^{(t)})$ ; then the worker nodes wait for the server to finish the proximal operation. This synchronization wastes much time and computational resources. Therefore, PARAMETERSERVER introduces a delayed proximal gradient updating method to implement asynchronous computation.

Specifically, we set a delay limit  $\tau \geq 0$ . At any iteration  $t$ , a worker does not need to wait until all the workers are fully synchronized. Instead, the worker will compute and push the local gradient to the server immediately if all the other workers have finished the iteration  $t - \tau$ . The server nodes will never wait to aggregate the gradients when a new gradient is received. The servers will perform the proximal update as long as all the gradients are within the delay limit  $\tau$ , i.e.,  $\nabla G^{(t)} = \sum_k \nabla G_k^{(t_k)}$ , where  $t - \tau \leq t_k \leq t$ . Obviously, this delay mechanism can effectively reduce the waiting time of server and worker nodes. By setting different  $\tau$ , we can adjust the degree of the asynchronous computation: when  $\tau = 0$ , we have no asynchronization and return to the standard proximal gradient descent; when  $\tau = \infty$ , we are totally asynchronous and there does not exist any waiting procedure.

A highlight is that given the composite form of the non-convex loss function in Equation (12), the above asynchronous delayed proximal gradient descent guarantees to converge according to Theorem 4.1.

**Theorem 4.1.** (Li et al., 2013) *Assume the gradient of the function  $G_k$  is Lipschitz continuous, that is, there is a constant  $C_k$  such that  $\|\nabla G_k(\boldsymbol{\theta}) - \nabla G_k(\boldsymbol{\theta}')\| \leq C_k \|\boldsymbol{\theta} - \boldsymbol{\theta}'\|$  for any  $\boldsymbol{\theta}, \boldsymbol{\theta}'$ , and  $k = 1, \dots, r$ . Define  $C = \sum_{k=1}^r C_k$ . Also, assume we allow a maximum delay for the updates by  $\tau$  and a significantly-modified filter on pulling the parameters with threshold  $\mathcal{O}(t^{-1})$ . For any  $\epsilon > 0$ , the delayed proximal gradient descent converges to a stationary point if the learning rate  $\gamma_t$  satisfies  $\gamma_t \leq ((1 + \tau)C + \epsilon)^{-1}$ .*

Now, we return to the discussion of our variational GP framework. A major benefit of our framework is that the negative variational lower bound of GP regression model has the same composite form as Equation (12). Thereby we can apply the asynchronous proximal gradient descent for GP inference in PARAMETERSERVER. Specifically, we explicitly assume  $q(\mathbf{w}) = \mathcal{N}(\mathbf{w}|\boldsymbol{\mu}, \boldsymbol{\Sigma})$  and obtain the negative variational ELBO (see Equation (10))

$$-\mathcal{L} = \sum_{i=1}^n g_i + h \quad (14)$$

where

$$\begin{aligned} g_i &= -\log \mathcal{N}(y_i | \boldsymbol{\phi}^\top(\mathbf{x}_i)\boldsymbol{\mu}, \beta^{-1}) + \frac{\beta}{2} \boldsymbol{\phi}^\top(\mathbf{x}_i)\boldsymbol{\Sigma}\boldsymbol{\phi}(\mathbf{x}_i) \\ &\quad + \frac{\beta}{2} \tilde{k}_{ii}, \\ h &= \frac{1}{2} (-\ln |\boldsymbol{\Sigma}| - m + \text{tr}(\boldsymbol{\Sigma}) + \boldsymbol{\mu}^\top \boldsymbol{\mu}). \end{aligned} \quad (15)$$

Instead of directly updating  $\boldsymbol{\Sigma}$ , we consider  $\mathbf{U}$ , the upper triangular Cholesky factor of  $\boldsymbol{\Sigma}$ , i.e.,  $\boldsymbol{\Sigma} = \mathbf{U}^\top \mathbf{U}$ . This not only simplifies the proximal operation but also ensures the positive definiteness of  $\boldsymbol{\Sigma}$  during computation. The partial derivative of  $g_i$  with respect to  $\boldsymbol{\mu}$  and  $\mathbf{U}$  are

$$\frac{\partial g_i}{\partial \boldsymbol{\mu}} = \beta (-y_i \boldsymbol{\phi}(\mathbf{x}_i) + \boldsymbol{\phi}(\mathbf{x}_i) \boldsymbol{\phi}^\top(\mathbf{x}_i) \boldsymbol{\mu}), \quad (16)$$

$$\frac{\partial g_i}{\partial \mathbf{U}} = \beta \text{triu}[\mathbf{U} \boldsymbol{\phi}(\mathbf{x}_i) \boldsymbol{\phi}^\top(\mathbf{x}_i)], \quad (17)$$

where  $\text{triu}[\cdot]$  denotes the operator that keeps the upper triangular part of a matrix but leaves any other element zero. It can be verified that the partial derivatives of  $g_i$  with respect to  $\boldsymbol{\mu}$  and  $\mathbf{U}$  are Lipschitz continuous and  $h$  is also convex with respect to  $\boldsymbol{\mu}$  and  $\mathbf{U}$ . According to Theorem 4.1, minimizing  $-\mathcal{L}$  (i.e., maximizing  $\mathcal{L}$ ) with respect to the variational parameters,  $\boldsymbol{\mu}$  and  $\mathbf{U}$ , using the asynchronous proximal gradient method can guarantee convergence. For other parameters, such as kernel parameters and inducing points,  $h$  is simply a constant. As a result, the delayed proximal updates for these parameters reduce to the delayed gradient descent optimization such as in (Agarwal and Duchi, 2011).

We now present the details of implementing ADVGP on PARAMETERSERVER. We first partition the data to  $r$  workers and allocate model parameters (such as kernel parameters, parameters of  $q(\mathbf{w})$  and inducing points  $\mathbf{Z}$ ) to server nodes. For each worker  $k$ , at any iteration  $t$ , as long as  $t - \tau$  previous iterations are finished on the server side, the worker  $k$  computes the gradient according to its data subset  $D_k$ ,  $\nabla G_k^{(t)} = \sum_{i \in D_k} \nabla g_i^{(t)}$ , and then pushes the gradient to the server nodes. The server nodes then aggregate the gradients and perform the proximal operation in Equation (13). Note that the proximal operation is only performed over the parameters of  $q(\mathbf{w})$ , namely  $\boldsymbol{\mu}$  and  $\mathbf{U}$ ; since  $h$  is constant for other model parameters, such as the kernel parameters and the inducing points, their gradient descent updates remain unchanged. Solving the minimization in Equation (13) by setting the derivatives to zero, we have the proximal updates for each element in  $\boldsymbol{\mu}$  and  $\mathbf{U}$  as

$$\mu_i^{(t+1)} = \mu_i'^{(t+1)} / (1 + \gamma_t), \quad (18)$$

$$U_{ij}^{(t+1)} = U_{ij}'^{(t+1)} / (1 + \gamma_t), \quad (19)$$

$$U_{ii}^{(t+1)} = \frac{U_{ii}'^{(t+1)} + \sqrt{(U_{ii}'^{(t+1)})^2 + 4(1 + \gamma_t)\gamma_t}}{2(1 + \gamma_t)}, \quad (20)$$

where

$$\mu_i'^{(t+1)} = \mu_i^{(t)} - \gamma_t \sum_{k=1}^r \frac{\partial G_k^{(t)}}{\partial \mu_i^{(t)}},$$

$$U_{ij}'^{(t+1)} = U_{ij}^{(t)} - \gamma_t \sum_{k=1}^r \frac{\partial G_k^{(t)}}{\partial U_{ij}^{(t)}}.$$

These proximal operations are element-wise, closed-form computations, therefore making the updates of the variational posterior  $q(\mathbf{w})$  highly parallelizable and efficient. Regarding the gradient calculation with respect to the other parameters, we give the details in the supplementary material (Appendix A). Finally, ADVGP is summarized in Algorithm 1.

## 5 Discussion and Related Work

Exact GP inference requires computing the full covariance matrix (and its inverse), and therefore is infeasible for large data. To reduce the computational cost, many approximation inference methods use a low-rank structure to approximate the full covariance. Those methods are called sparse GP, because the original dense computation in full covariance now becomes sparse due to the low-rank structure. Williams and Seeger (2001) used the Nyström approximation to speed up GPs. In sparse spectrum Gaussian process (SSGP), Lázaro-Gredilla *et al.* (2010) used truncated trigonometric expansions of the kernel function. A variant of sparse GPs introduced a small set of inducing inputs, viewed as statistical summary of the data, and define an approximate model by imposing some conditional independence between latent functions given the inducing points. The inference of the inexact model is thereby much easier. Quiñero-Candela and Rasmussen (2005) provided a unifying view of those methods, including subsets of regressors (SoR) (Smola and Bartlett, 2001), deterministic training conditional (DTC) (Seeger *et al.*, 2003), fully independent training conditional (FITC) (Snelson and Ghahramani, 2005) and partially independent conditional (PITC) (Schwaighofer and Tresp, 2003).

---

**Algorithm 1** Delayed Proximal Gradient for ADVGP

---

**Worker  $k$  at iteration  $t$** 

- 1: Block until server has a new parameter ready
- 2: Pull parameters from servers
- 3: Compute the gradient  $\nabla G_k^{(t)}$  on data  $D_k$  for kernel parameters and variational parameters
- 4: Push the gradient  $\nabla G_k^{(t)}$  to servers

**Servers at iteration  $t$** 

- 1: Update if every worker  $k$  completes iteration  $t_k \geq t - \tau$
  - 2: Aggregate gradients to obtain  $\nabla G^{(t)} = \sum \nabla G_k^{(t_j)}$
  - 3: Update  $\mu$  and  $U$  using (18), (19) and (20)
  - 4: Update other parameters using gradient descent
  - 5: Notify all blocked workers about the new parameters
- 

Despite the success of those methods, their inference procedures often exhibit undesirable behaviors, such as underestimation of the noise and clumped inducing inputs (Bauer *et al.*, 2016). To provide a rigorous approximation, Titsias (2009) proposed a variational sparse GP framework which can overcome those shortages. In the variational sparse GP framework, the approximate posteriors and the inducing points are both treated as variational parameters and estimated by maximizing a variational lower bound of the true model evidence. The variational framework is less prone to overfitting and often yields a better inference quality (Titsias, 2009; Bauer *et al.*, 2016). Based on Titsias (2009)’s work, Hensman *et al.* (2013) developed a stochastic variational inference for GP (SVIGP) by parameterizing the variational distributions explicitly. Gal *et al.* (2014) reparameterized the bound of Titsias (2009) and develop a distributed optimization algorithm with the MAPREDUCE framework. Further, Dai *et al.* (2014) developed a GPU acceleration using the similar formulation. Hoang *et al.* (2016) derived a distributed variational approximation for correlated noise.

To further enable GPs on real-world, extremely large applications, we proposed a new variational GP framework using a weight space augmentation. The proposed augmented model, however, is very different from the traditional weight space view of GP regression, where the weight vector is for the underlying nonlinear feature mapping brought by the covariance function and therefore could be infinite dimensional. In our framework, the dimension of the weight vector  $\mathbf{w}$  (i.e.,  $m$ ) is fixed and much smaller than the number of samples. The feature mapping  $\phi(\cdot)$  is used to construct a tractable variational lower bound, rather than describe the nonlinear feature mapping underlying the covariance function.

The advantages of our new framework are mainly twofold. First, by using a feature mapping  $\phi(\cdot)$ , we are flexible to incorporate different low rank structures, and meanwhile still cast them into a principled variational inference framework.

For example, in addition to Equation (11), we can define

$$\phi(\mathbf{x}) = \text{diag}(\lambda)^{-1/2} \mathbf{Q}^\top \mathbf{k}_m(\mathbf{x}), \quad (21)$$

where  $\mathbf{Q}$  are  $\lambda$  are eigenvectors and eigenvalues of  $\mathbf{K}_{mm}$ . Then  $\phi(\cdot)$  is actually a scaled Nyström approximation for eigenfunctions of the kernel used in GP regression.

A natural extension to using only one Nyström approximation for the eigenfunctions is to replace the feature mapping with a combination of  $q$  Nyström approximations. Suppose we have  $q$  groups of inducing inputs  $\{\mathbf{Z}_1, \dots, \mathbf{Z}_q\}$ , where each  $\mathbf{Z}_l$  consists of  $m_l$  inducing inputs. Then the feature mapping can be defined as

$$\phi(\mathbf{x}) = \sum_{l=1}^q q^{-1/2} \text{diag}(\lambda_l)^{-1/2} \mathbf{Q}_l^\top \mathbf{k}_{m_l}(\mathbf{x}), \quad (22)$$

where  $\lambda_l$  and  $\mathbf{Q}_l$  are the eigenvalues and eigenvectors of the covariance matrix for  $\mathbf{Z}_l$ . This leads to a variational sparse GP model based on the ensemble Nyström method (Kumar *et al.*, 2009). Using Equation (22), we can improve the variational ELBO without increasing the computation complexity for a small constant  $q > 1$ .

In addition, we can also relate ADVGP to GP models with pre-defined feature mappings, such as the Relevance Vector Machines (RVMs) (Bishop and Tipping, 2000) by setting  $\phi(\mathbf{x}) = \text{diag}(\boldsymbol{\alpha}^{1/2})\mathbf{k}_m(\mathbf{x})$ , where  $\boldsymbol{\alpha}$  is an  $m \times 1$  weight vector; and the SSGP (Lázaro-Gredilla *et al.*, 2010) by setting  $\phi(\mathbf{x}) = a_0 \exp(2\pi i \mathbf{x} \mathbf{S})$ , where  $i$  is the imaginary unit and  $\mathbf{S}$  is a  $d \times 2m$  matrix representing the sampled paired frequencies, namely the spectral points.

The second major advantage of ADVGP is that our variational ELBO is consistent with the composite non-convex loss form supported by PARAMETERSERVER, therefore we are able to utilize the highly efficient, asynchronous proximal gradient descent in PARAMETERSERVER to scale up GP models to applications with extremely large data volume. Furthermore, the simple element-wise and closed-form proximal operation enables highly efficient and parallelizable variational posterior update on the server side.

## 6 Experiments

### 6.1 Predictive Performance

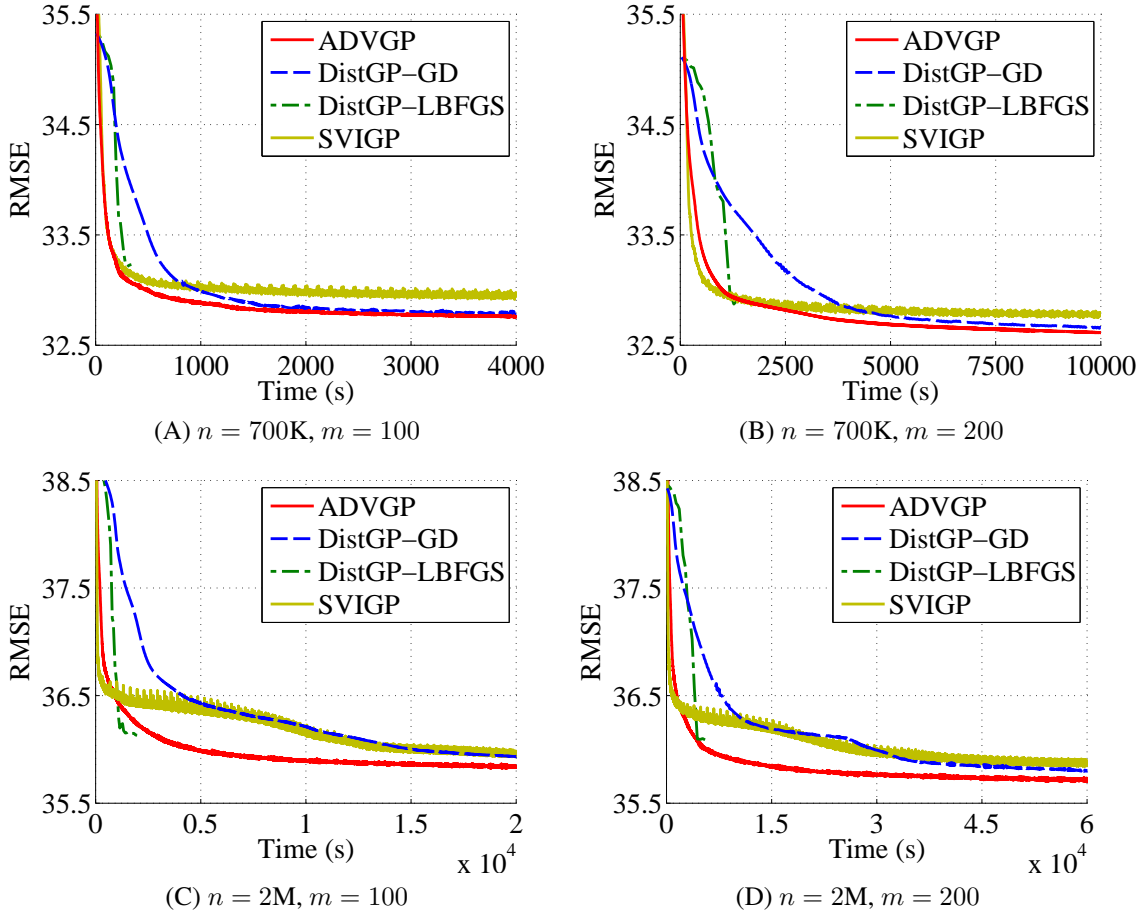


Figure 1: Root mean square errors for US flight data as a function of training time.



First, we evaluated the inference quality of ADVGP in terms of prediction performance. To this end, we used the US Flight data<sup>1</sup> (Hensman *et al.*, 2013), which recorded the arrival and departure time of the USA commercial flights between January and April in 2008. We performed two groups of tests: in the first group, we randomly chose 700K samples for training; in the second group, we randomly selected 2M training samples. Both groups used 100K samples for testing. We ensured that the training and testing data are non-overlapping.

We compared ADVGP with two existing scalable variational inference algorithms: SVIGP (Hensman *et al.*, 2013) and DistGP (Gal *et al.*, 2014). SVIGP employs online training, and DistGP performs a distributed synchronous variational inference. All the methods were reimplemented on a computer node with 16 CPU cores and 64 GB memory. While SVIGP uses a single CPU core, DistGP and ADVGP use all the CPU cores to perform parallel inference. We used ARD kernel for all the methods, with the same initialization of the kernel parameters. For SVIGP, we set the mini-batch size to 5000. For DistGP, we tested two optimization frameworks: local gradient descent (DistGP-GD) and L-BFGS (DistGP-LBFGS). For ADVGP, we initialized  $\mu = \mathbf{0}$ ,  $\mathbf{U} = \mathbf{I}$ , and used ADADELTA (Zeiler, 2012) to tune the step size for the gradient descent before the proximal operation. To choose an appropriate delay  $\tau$ , we sampled another subset from the training data, based on which we tuned the hyperparameter  $\tau$  from the set  $\{0, 8, 16, 24, 32, 40\}$ . Note that when  $\tau = 0$ , the computation is totally synchronous; larger  $\tau$  results in more asynchronous computation. We chose  $\tau = 32$  as it produced the best performance on the sampled subset.

Table 1 and Table 2 show the root mean square errors (RMSEs) of all methods for different numbers of inducing points, i.e.,  $m \in \{50, 100, 200\}$ . In these tables, ADVGP exhibits better or comparable predictive performance in all cases. These results show that by using an asynchronous computation process, ADVGP maintains the robustness for inference. Furthermore, we examined the predictive performance of each method along with the time by testing different settings:  $m \in \{100, 200\}$ . Figure 1 shows that during the same time span, ADVGP achieves the highest performance boost (i.e., RMSE is reduced faster than the competing methods), which demonstrates the efficiency of ADVGP. It is interesting to see that in a short period of time at the beginning, SVIGP reduces RMSE as fast as ADVGP; however, after that, RMSE of SVIGP is constantly larger than ADVGP, showing an inferior performance. In addition, DistGP-LBFGS converges earlier than both ADVGP and SVIGP. However, RMSE of DistGP-LBFGS is larger than both ADVGP and SVIGP at convergence. This implies that the L-BFGS optimization converged to a suboptimal solution.

Table 1: Root mean square errors for 700K/100K US Flight data.

Method	$m = 50$	$m = 100$	$m = 200$
Prox GP	<b>32.9080</b>	<b>32.7543</b>	<b>32.6143</b>
GD Dist GP	32.9411	32.8069	32.6521
LBFG Dist GP	33.0707	33.2263	32.8729
SVIGP	33.1054	32.9499	32.7802

Table 2: Root mean square errors for 2M/100K US Flight data.

Method	$m = 50$	$m = 100$	$m = 200$
Prox GP	36.1156	<b>35.8347</b>	<b>35.7017</b>
GD Dist GP	36.0142	35.9487	35.7971
LBFG Dist GP	<b>35.9809</b>	36.1676	36.0749
SVIGP	36.2019	35.9517	35.8599

We also studied how the delay limit  $\tau$  affects the performance of ADVGP. In practice when many machines are used, some worker may always be slower than the others due to environmental factors, for ex-

<sup>1</sup><http://stat-computing.org/dataexpo/2009/>

ample, unbalanced workloads. To simulate this scenario, we intentionally introduced a latency by assigning each worker a random sleep time of 0, 10 or 20 seconds on initialization, hence a worker would pause for its given sleep time at each iteration. The average per-iteration running time for a worker was only 0.176 seconds in our experiment, so the fastest worker could be hundreds of iterations ahead of the slowest one in the asynchronous setting. We set  $\tau = 0, 5, 10, 20, 40, 80, 160$  and kept other parameters the same and plotted RMSEs as a function of time for each delay limit  $\tau$  in Figure 2. Since RMSE of the synchronous case ( $\tau = 0$ ) is much larger than the others, it is not shown in the figure. As shown in the figure, when  $\tau$  is larger, ADVGP behaves more stochastically. By increasing  $\tau$ , we first achieved a better performance owing to the CPU utilization, however later we observed a decrease in performance due to the stochastic behavior. Therefore, in order to use ADVGP for workers at very different paces, a good delay limit  $\tau$  needs to be chosen carefully.

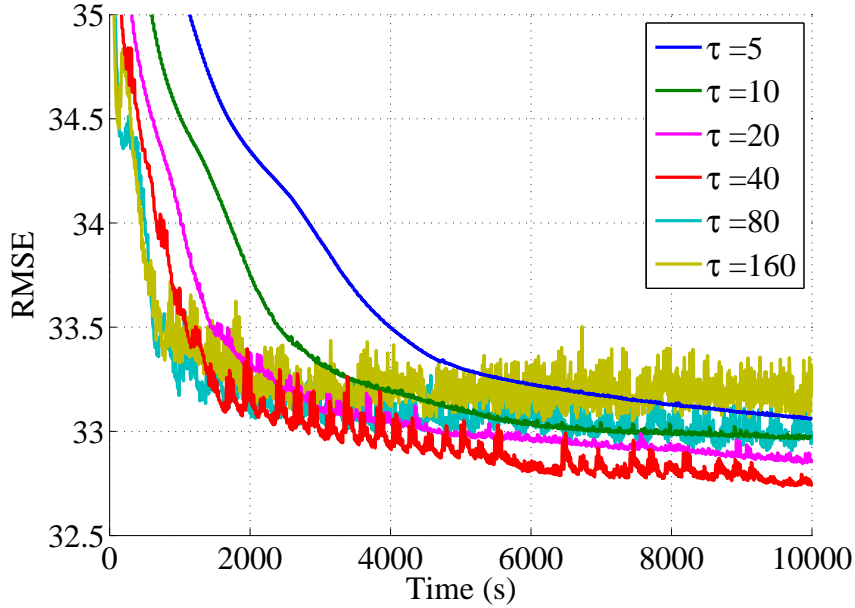


Figure 2: Root mean square errors as a function of time for different delay limits  $\tau$

## 6.2 Scalability

Next, we examined the scalability of the proposed asynchronous GP inference method, ADVGP. To this end, we used the 700K/100K dataset and compared with the synchronous inference algorithm DistGP (Gal *et al.*, 2014). For a fair comparison, we used the local gradient descent version of DistGP, i.e., DistGP-GD. We conducted two experiments by setting the number of inducing points  $m = 100$ . In the first experiment, we fixed the size of the training data, and increased the number of CPU cores from 4 to 128. We examined the per-iteration running time of both ADVGP and DistGP-GD. Figure 3(A) shows that while both decreasing with more CPU cores, the per-iteration running time of ADVGP is much less than that of DistGP-GD. This demonstrates the advantage of the asynchronous inference in computational efficiency. On the other hand, the decreasing of the per-iteration running time of DistGP-GD decays much more quickly than that of ADVGP as the number of cores approaches 128. This demonstrates that as the communication cost becomes a dominant factor influencing computing, the asynchronous updates of ADVGP can help reduce the latency. In the second experiment, we increased both the number of cores and the size of training data. We started from 87.5K samples and 16 cores and gradually increased them to 700K samples and 128 cores. As

shown in Figure 3(B), the average per-iteration time of DistGP-GD grows linearly to the size of data; however, the average per-iteration time of ADVGP stays almost constant. We deduce that without synchronous coordination, ADVGP can fully utilize the network bandwidth so that the increased amount of messages along with the growth of the data size affect little the efficiency of network communication. This as well illustrates the advantage of asynchronous inference, from another perspective, in communication efficiency.

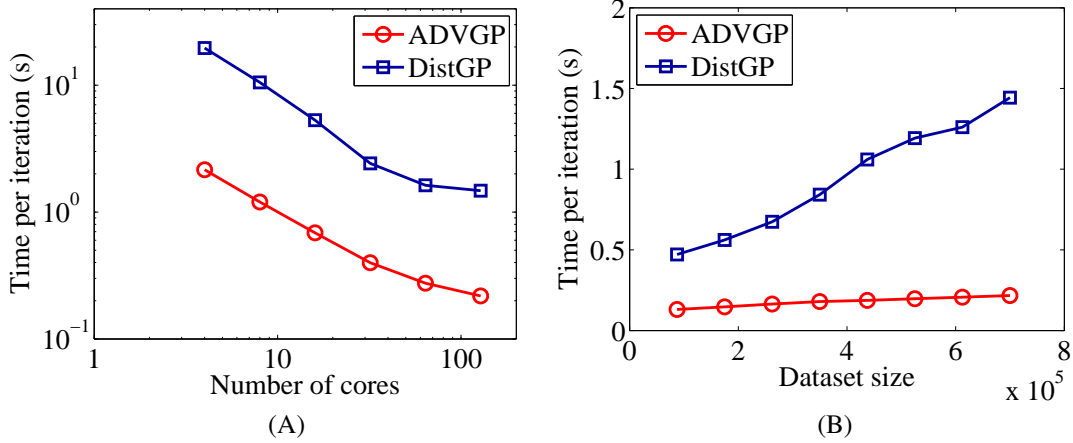


Figure 3: Scalability tests on 700K US flight data. (A) Per-iteration time as a function of available cores in log-scale. (B) Per-iteration time when scaling the computational resources proportionally to dataset size.

### 6.3 NYC Taxi Traveling Time Prediction

Finally, we applied ADVGP for an extremely large problem: the prediction of the taxi traveling time in New York city. We used the New York city yellow taxi trip dataset<sup>2</sup>, which consist of 1.21 billions of trip records from January 2009 to December 2015. We excluded the trips that are outside the NYC area or more than 5 hours. The average traveling time is 764 seconds and the standard derivation is 576 seconds. To predict the traveling time, we used the following 9 features: time of the day, day of the week, day of the month, month, pick-up latitude, and pick-up longitude, drop-off latitude, drop-off longitude, and travel distance. We ran ADVGP on multiple Amazon c4.8xlarge instances each with 36 vCPUs and 60 GB memory. We compared with the linear regression model implemented in Vowpal Wabbit (Agarwal *et al.*, 2014). Note that Vowpal Wabbit is a state-of-the-art large scale machine learning software package and has been used in many industrial-scale applications, such as click-through-rate prediction (Chapelle *et al.*, 2014).

We first randomly selected 100M training samples and 500K test samples. We used  $m = 50$  as the number of inducing points, which are initialized by performing the K-means clustering on a subset of 2M training samples. We trained a GP regression model with ADVGP, using 5 Amazon instances with 200 processes. The delay limit is selected as  $\tau = 20$ . And we trained a linear regression model using Vowpal Wabbit with default settings. In Figure 4(A), we report RMSEs of the GP regression and the linear regression along with time. We also simply took the average traveling time over the training data as the mean prediction. As we see, during the same running time, the nonlinear regression model trained by ADVGP greatly outperforms the linear model in terms of prediction accuracy.

To further verify the advantage of GP regression in applications of extremely large scale data, we used 1B samples for training and 1M samples for testing. We used 50 inducing points, initialized by the K-means cluster centers from a 1M training data subset. We ran ADVGP using 28 Amazon instances with 1000 processes and the delay limit is chosen as  $\tau = 100$ . As shown in Figure 4(B), the RMSE of GP regression

<sup>2</sup>[http://www.nyc.gov/html/tlc/html/about/trip\\_record\\_data.shtml](http://www.nyc.gov/html/tlc/html/about/trip_record_data.shtml)

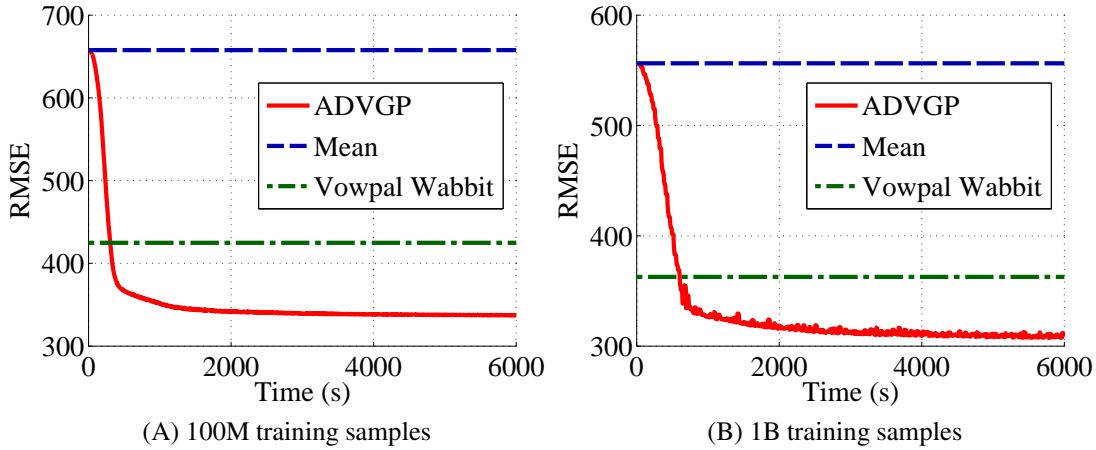


Figure 4: Root mean square errors as a function of training time on NYC Taxi Data.

outperforms the linear model by a large margin. These results confirm the power of our nonlinear model ADVGP in even larger scenarios, comparing with linear models. Additionally, in terms of running speed, the average per-iteration time of ADVGP is only 0.21 seconds.

## 7 Conclusion

We have presented ADVGP, an asynchronous, distributed variational inference algorithm for GP regression, based on a novel variational GP framework with weighted space augmentation. The weight space argumentation provides a very flexible framework for different variational lower bounds and relates many sparse GP models. More importantly, ADVGP greatly improves the scalability of GPs and enables extremely large applications, say, with billions of training samples. In the future, we plan to further explore various feature mappings in our framework, to construct different variational evidence lower bounds and examine their performance in real-world applications.

## References

- Agarwal, A. and Duchi, J. C. (2011). Distributed delayed stochastic optimization. In *Advances in Neural Information Processing Systems 24*, pages 873–881. The MIT Press.
- Agarwal, A., Chapelle, O., Dudík, M., and Langford, J. (2014). A reliable effective terascale linear learning system. *Journal of Machine Learning Research*, **15**, 1111–1133.
- Bauer, M., van der Wilk, M., and Rasmussen, C. E. (2016). Understanding probabilistic sparse Gaussian process approximations. In *Advances in Neural Information Processing Systems 29*, pages 1525–1533.
- Bishop, C. M. and Tipping, M. E. (2000). Variational relevance vector machines. In *Proceedings of the 16th Conference in Uncertainty in Artificial Intelligence (UAI)*.
- Chapelle, O., Manavoglu, E., and Rosales, R. (2014). Simple and scalable response prediction for display advertising. *ACM Transactions on Intelligent Systems and Technology (TIST)*, **5**(4), 61:1–61:34.
- Dai, Z., Damianou, A., Hensman, J., and Lawrence, N. D. (2014). Gaussian process models with parallelization and GPU acceleration. In *NIPS Workshop on Software Engineering for Machine Learning*.
- Deisenroth, M. and Ng, J. W. (2015). Distributed Gaussian processes. In *Proceedings of the 32nd International Conference on Machine Learning*, pages 1481–1490.

- Gal, Y., van der Wilk, M., and Rasmussen, C. E. (2014). Distributed variational inference in sparse Gaussian process regression and latent variable models. In *Advances in Neural Information Processing Systems 27*, pages 3257–3265.
- Hensman, J., Fusi, N., and Lawrence, N. D. (2013). Gaussian processes for big data. In *Proceedings of the Conference on Uncertainty in Artificial Intelligence (UAI)*.
- Hoang, T. N., Hoang, Q. M., and Low, B. K. H. (2016). A distributed variational inference framework for unifying parallel sparse Gaussian process regression models. In *Proceedings of the 33rd International Conference on Machine Learning*, pages 382–391.
- Kumar, S., Mohri, M., and Talwalkar, A. (2009). Ensemble Nyström method. In Y. Bengio, D. Schuurmans, J. D. Lafferty, C. K. I. Williams, and A. Culotta, editors, *Advances in Neural Information Processing Systems 22*, pages 1060–1068.
- Lázaro-Gredilla, M., Quiñero-Candela, J., Rasmussen, C. E., and Figueiras-Vidal, A. R. (2010). Sparse spectrum Gaussian process regression. *Journal of Machine Learning Research*, **11**, 1865–1881.
- Li, M., Andersen, D. G., and Smola, A. J. (2013). Distributed delayed proximal gradient methods. In *NIPS Workshop on Optimization for Machine Learning*.
- Li, M., Andersen, D. G., Smola, A. J., and Yu, K. (2014a). Communication efficient distributed machine learning with the parameter server. In *Neural Information Processing Systems 27*, pages 19–27.
- Li, M., Andersen, D. G., Park, J. W., Smola, A. J., Ahmed, A., Josifovski, V., Long, J., Shekita, E. J., and Su, B.-Y. (2014b). Scaling distributed machine learning with the parameter server. In *11th USENIX Symposium on Operating Systems Design and Implementation (OSDI 14)*, pages 583–598.
- Quiñero-Candela, J. and Rasmussen, C. E. (2005). A unifying view of sparse approximate Gaussian process regression. *The Journal of Machine Learning Research*, **6**, 1939–1959.
- Rasmussen, C. E. and Williams, C. K. I. (2006). *Gaussian Processes for Machine Learning*. The MIT Press.
- Schwaighofer, A. and Tresp, V. (2003). Transductive and inductive methods for approximate Gaussian process regression. In *Advances in Neural Information Processing Systems 15*, pages 953–960. The MIT Press.
- Seeger, M., Williams, C., and Lawrence, N. (2003). Fast forward selection to speed up sparse Gaussian process regression. In *Proceedings of the Ninth International Workshop on Artificial Intelligence and Statistics*.
- Smola, A. J. and Bartlett, P. L. (2001). Sparse greedy Gaussian process regression. In *Advances in Neural Information Processing Systems 13*, pages 619–625. The MIT Press.
- Snelson, E. and Ghahramani, Z. (2005). Sparse Gaussian processes using pseudo-inputs. In *Advances in Neural Information Processing Systems*, pages 1257–1264.
- Titsias, M. K. (2009). Variational learning of inducing variables in sparse Gaussian processes. In *Proceedings of the 12th International Conference on Artificial Intelligence and Statistics*, pages 567–574. Journal of Machine Learning Research Workshop and Conference Proceedings.
- Williams, C. and Seeger, M. (2001). Using the Nyström method to speed up kernel machines. In *Advances in Neural Information Processing Systems 13*, pages 682–688.
- Zeiler, M. D. (2012). ADADELTA: an adaptive learning rate method. *arXiv1212.5701*.

# Appendices

## A Derivatives

### A.1 Objective

As described in the paper, the objective function to be minimized is  $-\mathcal{L} = \sum_{i=1}^n g_i + h$ , where

$$\begin{aligned} g_i &= -\ln \mathcal{N}(y_i | \phi_i^T \boldsymbol{\mu}, \beta^{-1}) + \frac{\beta}{2} \phi_i^T \boldsymbol{\Sigma} \phi_i + \frac{\beta}{2} \tilde{k}_{ii} \\ &= \frac{1}{2} \ln 2\pi - \frac{1}{2} \ln \beta + \frac{\beta}{2} (y_i^2 - 2y_i \phi_i^T \boldsymbol{\mu} + \boldsymbol{\mu}^T \phi_i \phi_i^T \boldsymbol{\mu} + \phi_i^T \boldsymbol{\Sigma} \phi_i + k_{ii} - \phi_i^T \phi_i), \end{aligned} \quad (23)$$

$$\begin{aligned} h &= \text{KL}(q(\mathbf{w}) || p(\mathbf{w})) \\ &= \frac{1}{2} (-\ln |\boldsymbol{\Sigma}| - m + \text{tr}(\boldsymbol{\Sigma}) + \boldsymbol{\mu}^T \boldsymbol{\mu}), \end{aligned} \quad (24)$$

and we define  $\beta = \sigma^{-2}$  and  $\phi_i = \phi(\mathbf{x}_i)$ .

### A.2 Kernel

A common choice for the kernel is the anisotropic squared exponential covariance function:

$$k(\mathbf{x}_i, \mathbf{x}_j) = a_0^2 \exp \left( -\frac{1}{2} (\mathbf{x}_i - \mathbf{x}_j)^T \text{diag}(\boldsymbol{\eta}) (\mathbf{x}_i - \mathbf{x}_j) \right), \quad (25)$$

in which the hyperparameters are the signal variance  $a_0$  and the lengthscales  $\boldsymbol{\eta} = \{1/a_k^2\}_{k=1}^d$ , controlling how fast the covariance decays with the distance between inputs. Using this covariance function, we can prune input dimensions by shrinking the corresponding lengthscales based on the data (when  $\eta_d = 0$ , the  $d$ -th dimension becomes totally irrelevant to the covariance function value). This pruning is known as Automatic Relevance Determination (ARD) and therefore this covariance is also called the ARD squared exponential.

#### Derivative over $\ln \sigma$

The derivative of  $g_i$  over  $\ln \sigma$  is

$$\frac{\partial g_i}{\partial \ln \sigma} = 1 - \frac{1}{\sigma^2} (y_i^2 - 2y_i \phi_i^T \boldsymbol{\mu} + \phi_i^T (\boldsymbol{\Sigma} + \boldsymbol{\mu} \boldsymbol{\mu}^T) \phi_i + k_{ii} - \phi_i^T \phi_i). \quad (26)$$

#### Derivative over $\ln a_0$

The derivative of  $g_i$  over  $\ln a_0$  is

$$\frac{\partial g_i}{\partial \ln a_0} = \frac{1}{\sigma^2} (-y_i \phi_i^T \boldsymbol{\mu} + \phi_i^T (\boldsymbol{\Sigma} + \boldsymbol{\mu} \boldsymbol{\mu}^T) \phi_i + k_{ii} - \phi_i^T \phi_i). \quad (27)$$

#### Derivative over $\mathbf{Z}$

By defining  $\mathbf{L}$  the lower triangular Cholesky factor of  $\mathbf{K}_{mm}^{-1}$ , the derivative of  $g_i$  over  $\mathbf{Z}$  is

$$\begin{aligned} \frac{\partial g_i}{\partial \mathbf{Z}} &= \frac{1}{\sigma^2} [ ((\mathbf{L} \mathbf{p}_i) \circ \mathbf{k}_m(\mathbf{x}_i)) \mathbf{x}_i^T \text{diag}(\boldsymbol{\eta}) - (((\mathbf{L} \mathbf{p}_i) \circ \mathbf{k}_m(\mathbf{x}_i)) \mathbf{1}_d^T) \circ (\mathbf{Z} \text{diag}(\boldsymbol{\eta})) \\ &\quad - (\mathbf{T}_i + \mathbf{T}_i^T) \mathbf{Z} \text{diag}(\boldsymbol{\eta}) + ((\mathbf{T}_i + \mathbf{T}_i^T) \mathbf{1}_m \boldsymbol{\eta}^T) \circ \mathbf{Z} ], \end{aligned} \quad (28)$$

where

$$\mathbf{p}_i = -\boldsymbol{\mu} y_i + (\boldsymbol{\mu} \boldsymbol{\mu}^T + \boldsymbol{\Sigma}) \phi(\mathbf{x}_i) - \phi(\mathbf{x}_i), \quad (29)$$

$$\mathbf{T}_i = [\mathbf{L} ((\phi(\mathbf{x}_i) \mathbf{p}_i^T) \circ \boldsymbol{\Psi}) \mathbf{L}^T] \circ \mathbf{K}_{mm}. \quad (30)$$

The symbol  $\circ$  denotes the Hadamard product, and  $\Psi$  is an upper triangular matrix with diagonal elements all equal to 0.5 and strictly upper triangular elements all equal to 1, as follows:

$$\Psi = \begin{bmatrix} 0.5 & 1 & \dots & 1 & 1 \\ 0 & 0.5 & \ddots & 1 & 1 \\ \vdots & \ddots & \ddots & \ddots & \vdots \\ 0 & 0 & \ddots & 0.5 & 1 \\ 0 & 0 & \dots & 0 & 0.5 \end{bmatrix}. \quad (31)$$

#### Derivative over $\ln \eta$

The derivative of  $g_i$  over  $\ln \eta$  is

$$\begin{aligned} \frac{\partial g_i}{\partial \ln \eta} = \frac{1}{2\sigma^2} \Big\{ & 2\mathbf{1}_m^T [Z \circ ((L\mathbf{p}_i) \circ \mathbf{k}_m(\mathbf{x}_i)) \mathbf{x}_i^T] - \mathbf{1}_m^T ((L\mathbf{p}_i) \circ \mathbf{k}_m(\mathbf{x}_i)) (\mathbf{x}_i \circ \mathbf{x}_i)^T \\ & - ((L\mathbf{p}_i) \circ \mathbf{k}_m(\mathbf{x}_i))^T (Z \circ Z) - \mathbf{1}_m^T [Z \circ ((T_i + T_i^T)Z)] + \mathbf{1}_m^T [(T_i + T_i^T)(Z \circ Z)] \Big\} \circ \eta. \end{aligned} \quad (32)$$

## B Properties of the ELBO of ADVGP

By defining  $U$  as the upper triangular Cholesky factor of  $\Sigma$ , i.e.,  $\Sigma = U^T U$ , we have

**Lemma B.1.** *The gradient of  $g_i$  in Equation 23,  $\nabla g_i$ , is Lipschitz continuous with respect to each element in  $\mu$  and  $U$ .*

We can prove this by showing the first derivative of  $\nabla g_i$  with respect to each element of  $\mu$  and  $U$  is bounded, which is constant in our case. As shown in our paper, the gradients of  $g_i$  with respect to  $\mu$  and  $U$  are:

$$\frac{\partial g_i}{\partial \mu} = \frac{1}{\sigma^2} [-y_i \phi_i + \phi_i \phi_i^T \mu], \quad (33)$$

$$\frac{\partial g_i}{\partial U} = \frac{1}{\sigma^2} \text{triu}[U \phi_i \phi_i^T], \quad (34)$$

which are affine functions for  $\mu$  and  $\Sigma$  respectively. Therefore, the first derivative of  $\nabla g_i$  is constant.

**Lemma B.2.**  *$h$  in Equation 24 is a convex function with respect to  $\mu$  and  $U$ .*

This can be proved by verifying that the Hessian matrices of  $h$  with respect to  $\mu$  and  $\text{vec}(U)$  are both positive semidefinite, where we denote  $\text{vec}(\cdot)$  as the operator that stacks the columns of a matrix as a vector. To show this, we first compute the partial derivatives of  $h$  with respect to  $\mu$  and  $U$  as

$$\frac{\partial h}{\partial \mu} = \mu, \quad (35)$$

$$\frac{\partial h}{\partial U} = -\text{diag}(U^{-1}) + U. \quad (36)$$

The Hessian matrix of  $h$  with respect to  $\mu$  is

$$\mathbf{H}(\mu) = \mathbf{I}_{m \times m} \succeq 0. \quad (37)$$

The Hessian matrix of  $h$  with respect to  $\text{vec}(U)$  is

$$\mathbf{H}(\text{vec}(U)) = \text{diag}(\mathbf{h}) \succeq 0, \quad (38)$$

where  $\mathbf{h} = [\frac{\partial h}{\partial U_{11}^2}, \dots, \frac{\partial h}{\partial U_{1m}^2}, \dots, \frac{\partial h}{\partial U_{m1}^2}, \dots, \frac{\partial h}{\partial U_{mm}^2}]$ , and  $\frac{\partial h}{\partial U_{ij}^2} = 1 + \delta(i, j) \frac{1}{U_{i,i}^2}$ .

## C Negative Log Evidences on US Flight Data

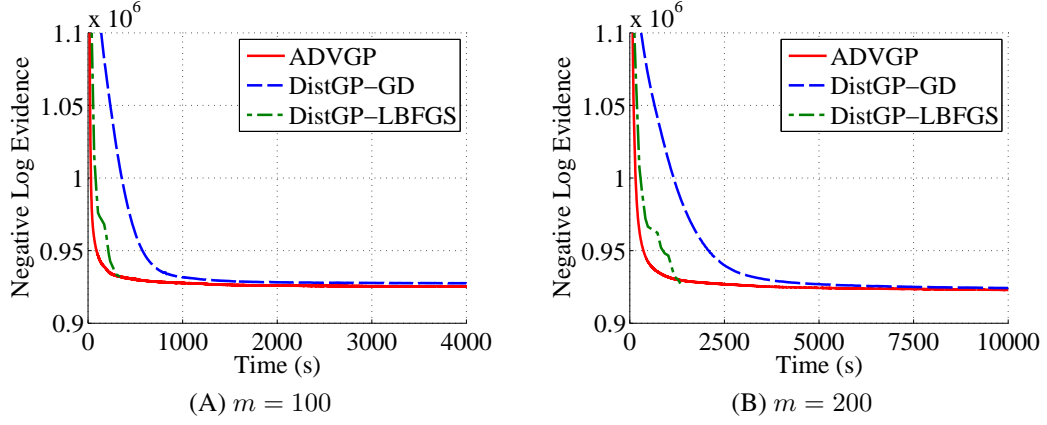


Figure C.1: Negative log evidences for 700K/100K US Flight data as a function of training time.

Method	$m = 100$	$m = 200$
ADVGP	<b>925236</b>	<b>922907</b>
DistGP-GD	927414	924208
DistGP-LBFGS	932179	927331

Table C.1: Negative log evidences for 700K/100K US Flight data.

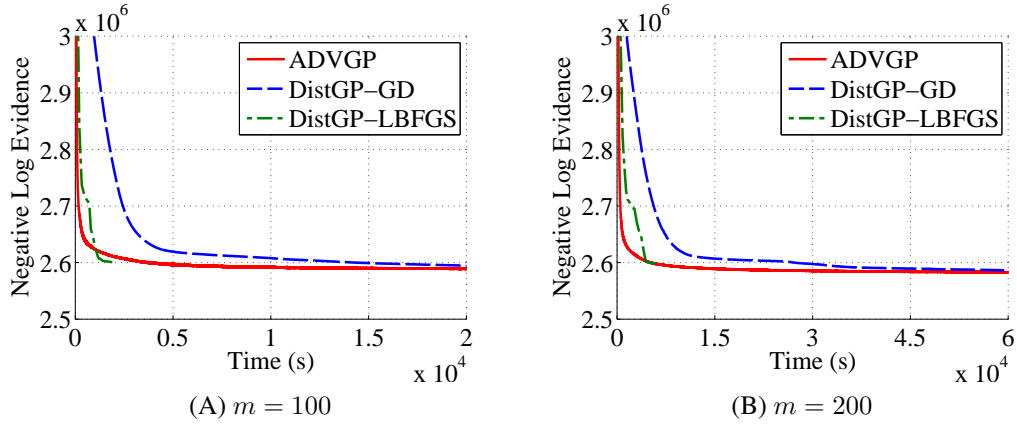


Figure C.2: Negative log evidences for 2M/100K US Flight data as a function of training time.

Method	$m = 100$	$m = 200$
ADVGP	<b><math>2.58921 \times 10^6</math></b>	<b><math>2.58267 \times 10^6</math></b>
DistGP-GD	$2.59471 \times 10^6$	$2.58601 \times 10^6$
DistGP-LBFGS	$2.59971 \times 10^6$	$2.59817 \times 10^6$

Table C.2: Negative log evidences for 2M/100K US Flight data.



## D Mean Negative Log Predictive Likelihoods (MNLPs) on US Flight Data

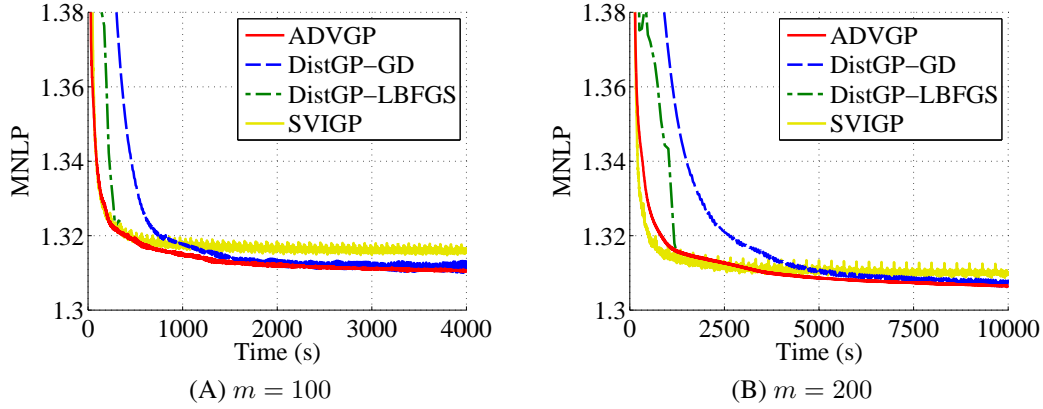


Figure D.1: Mean negative log predictive likelihoods for 700K/100K US Flight data as a function of training time.

Method	$m = 100$	$m = 200$
ADVGP	1.3106	1.3066
DistGP-GD	<b>1.3099</b>	<b>1.3062</b>
DistGP-LBFGS	1.3237	1.3136
SVIGP	1.3157	1.3096

Table D.1: Mean negative log predictive likelihoods for 700K/100K US Flight data.

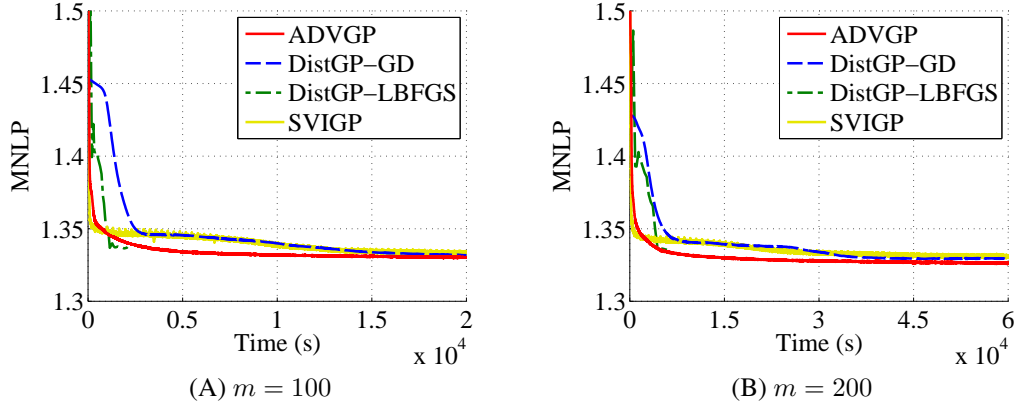


Figure D.2: Mean negative log predictive likelihoods for 2M/100K US Flight data as a function of training time.

Method	$m = 100$	$m = 200$
ADVGP	<b>1.3301</b>	<b>1.3258</b>
DistGP-GD	1.3317	1.3297
DistGP-LBFGS	1.3380	1.3355
SVIGP	1.3335	1.3306

Table D.2: Mean negative log predictive likelihoods for 2M/100K US Flight data.